Electronic structure of rare-earth hexaborides

S. Kimura
Research Institute for Scientific Measurements, Tohoku University, 2-1-1 Katahira, Aoba-ku, Sendai 980, Japan

T. Nanba and M. Tomikawa
Department of Physics, Faculty of Science, Kobe University, 1-1 Rokkodai, Nada-ku, Kobe 657, Japan

S. Kunii and T. Kasuya
Department of Physics, Faculty of Science, Tohoku University, Aramaki Aza Aoba, Aoba-ku, Sendai 980, Japan
(Received 24 February 1992)

Reflectivity spectra of all rare-earth hexaboride RB_6 (R = La, Ce, Pr, Nd, Sm, Eu, Gd, Tb, Dy, Ho, Yb, and Y) single crystals have been measured systematically in the energy region from 1 meV to 40 eV at 300 K in order to investigate the electronic state and the contribution of the $4f$ electron to the band structure. The analysis of the optical conductivity and the loss-function spectra, which were derived from the Kramers-Kronig transformation of the reflectivity spectra, allowed us to make clear the origin of the peak structure in the spectrum due to the various interband transitions. The origins of the main peaks in the spectrum were assigned to the interband transitions from the bonding to the antibonding bands of the boron $2s$ and $2p$ states and to the rare-earth $5d$ state. The intra-atomic transition from the $4f$ and the $5p$ to the $5d(t_{2g})$ states in the rare-earth ion was also observed.

I. INTRODUCTION

Rare-earth hexaborides (RB_6) are a series of the material group in which SmB_6 shows the valence fluctuation[1] and CeB_6 shows the dense Kondo effect.[2] These are intrinsic properties due to the $4f$ electron included in these materials. RB_6 forms a CaB_6-type crystal structure which belongs to the space group $P_m4_m(O_h)$.

Trivalent RB_6's are one-carrier metals because the B_6 octahedron bonding orbits are filled with two more electrons,[3] but the characters of SmB_6, EuB_6, and YbB_6 are different from that of other materials. The valence of the Sm ion in SmB_6 becomes 2.6–2.7 because of a valence fluctuation (mixed valence) material as mentioned above. Therefore the conduction-electron number of this material is thought to be 0.6–0.7. On the other hand, EuB_6 and YbB_6 are semiconductors because the rare-earth ion in these compounds is divalent.

Because these materials show various intersting properties, the electric, magnetic, and thermal properties have been widely investigated by many groups. However, their optical properties have been studied very little, except for SmB_6 by Travaglini and Wachter[4] which has a small gap structure close to the Fermi level only at low temperature. In the previous experiment, we have measured reflectivity spectra of only lighter RB_6, LaB_6, CeB_6, PrB_6, NdB_6, SmB_6, EuB_6, and GdB_6, in the energy region from 1 meV to 25 eV, and we have analyzed the origin of the peak structures in optical conductivity spectra derived from the reflectivity spectra by the Kramers-Kronig (KK) transformation.[5,6] On LaB_6, we have calculated the spectrum of the joint density of states (JDOS) and the partial JDOS, which are equivalent to the optical absorption, by using the result of the energy-band calculation by Harima *et al.*[7] and compared to the optical conductivity spectrum.[8] In these previous studies, we have made clear the origin of the structures in the optical spectrum which is given by the intra-atomic transition from the rare-earth $4f$ to the rare-earth $5d$ states in SmB_6 and GdB_6 and the charge-transfer excitation from the B_6 $2s$ and $2p$ bonding to the rare-earth $5d$ states in all materials.[5,8] We have found that the material containing $4f$ electron gives the anomalous infrared absorption at about 0.6 eV which is caused by the low-energy excitation of the conduction electron.[6] However, no optical measurement of heavier RB_6 has yet been done. We measured reflectivity spectra of TbB_6, DyB_6, HoB_6, YbB_6, and YB_6 single crystals the first time in addition to previously studied materials in the wider energy region from 1 meV to 40 eV. In the low-energy part below 2 eV, the interesting absorption structure due to the conduction electron and to the low-energy excitation was observed. For example, the energy gap and the absorption structure due to the occupied and unoccupied $4f$ states located near the Fermi level were seen in SmB_6 at a temperature below 20 K.[9] However, a detailed analysis of the conduction-electron absorption structure is made in a separate paper.[10] The main purpose of this paper is to develop our previous work[5] on the interband transition spectra to the heavier RB_6 and to understand totally the electronic structure of RB_6.

II. EXPERIMENT AND ANALYSIS

A. Sample preparation

All samples were grown to single crystals by the floating zone method.[11] The obtained crystals were cut into disks with about 7 mm in diameter and 1 mm in thick-

ness by an electric spark cutter and polished to mirror surface with carborundum and alumina powders for the reflectivity measurement.

B. Reflectivity measurement method

We measured the reflectivity spectrum in the wide energy range from 1 meV in the far-infrared region to 40 eV in the vacuum-ultraviolet region. The measurements in the far-infrared region from 1 to 30 meV and in the vacuum-ultraviolet region from 4 to 40 eV were done at two synchrotron radiation (SR) facilities, UVSOR at the Institute for Molecular Science and SOR-RING at the Institute for Solid State Physics, the University of Tokyo, respectively. In the former, the SR light was monochromatized by a Martin-Paplett–type Fourier spectrometer from Specac Ltd. and its intensity was detected by Ge and InSb bolometers from Infrared Laboratories, Inc.[12] In the latter, the SR was monochromatized by a 1-m Seya-Namioka–type monochromator from Kohzu Ltd. and its intensity was detected by photomultipliers from Hamamatsu Photonics Ltd.

For the measurement in the intermediate-energy region between 50 meV and 5 eV, appropriate combinations of conventional light sources, monochromators (a prism double monochromator from Carl Leiss Ltd. and a single-plane grating infrared monochromator from Hitachi Ltd.), and detectors were adopted. The spectra obtained by different spectrometers were connected smoothly. The expermental error of the absolute value of the reflectivity was estimated at less than 3% in the energy region above 2 eV.

The energy resolution ($E/\Delta E$) was higher than 20 at each energy. The measurements were both done at 80 and 300 K in the energy region above 2 eV, but the reflectivity spectra at both temperatures did not show any significant difference from each other. Therefore we discuss the reflectivity spectra only at 300 K in this paper.

C. Analysis method

Figure 1 shows the whole reflectivity spectra of all materials. In this figure, the energy position of the plasma edge of trivalent RB_6 and SmB_6 can be seen as a sharp decrease structure in the spectrum at about 2 eV, but those of EuB_6 and YbB_6 are located at a much lower energy than those of the other materials. This fact means that the number of the conduction electrons in EuB_6 and YbB_6 is smaller than that of the other trivalent RB_6 because of their semiconductorlike character.

In this paper, we consider the electronic states through the analysis of the optical conductivity and the loss-function spectra. The optical conductivity [$\sigma(\omega)=\omega\varepsilon_2/4\pi$; ε_2 is an imaginary part of the dielectric constant] and the loss-function [$-\mathrm{Im}(1/\varepsilon)$; ε shows the complex dielectric constant] spectra were obtained using the KK transformation of the reflectivity spectra. The KK transformation requires a reflectivity spectrum for a wide range of photon energy from zero frequency to infinity in principle.[13] Then we adopted two kinds of extrapolation functions in the energy region below 1 meV and above 40 eV. In the energy region below 1 meV, we

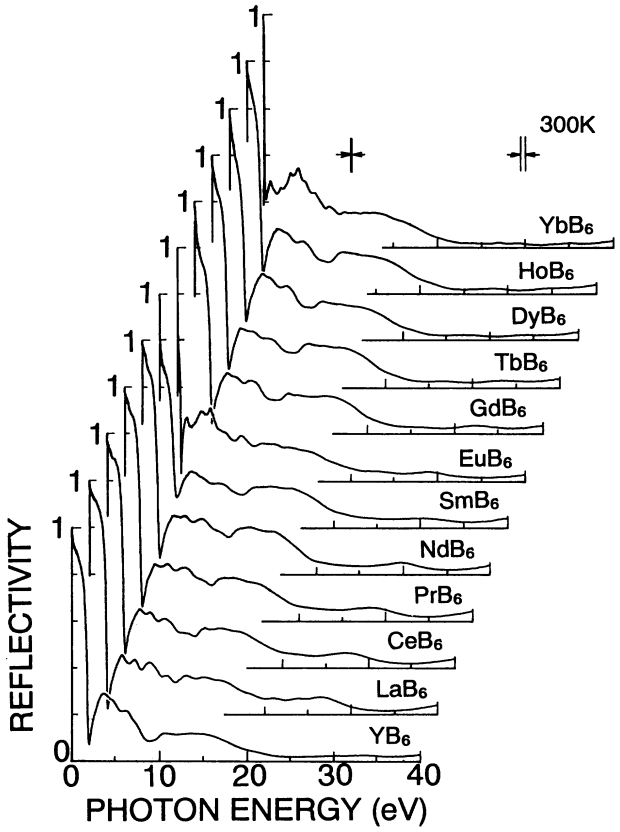

FIG. 1. Reflectivity spectra of all rare-earth hexaborides RB_6 (R=Y, La, Ce, Pr, Nd, Sm, Eu, Gd, Tb, Dy, Ho, and Yb) in the energy region from 1 meV to 40 eV at 300 K. The energy resolutions at 10 and 30 eV were 0.06 and 0.5 eV, respectively, and are indicated by the vertical double lines.

adopted a Hagen-Rubens function, $R(\omega)=1-A\omega^{1/2}$,[13] because of the metallic reflectivity spectrum. Here, $A=[\pi\sigma(0)/2]^{-1/2}$ and $\sigma(0)$ is the conductivity at zero frequency. In this case, we adopted the dc conductivity by the transport measurement as $\sigma(0)$. In the energy region above 40 eV, we adopted the usual extrapolation function for the electronic interband transition $R(\omega)=B\omega^{-4}$.[14] Here, we decided on the constant B so that the extrapolation functions connect with the actual reflectivity spectra. In this case, the typical B value was 1×10^5 eV^4.

Figures 2 and 4 show the optical conductivity spectra and Figs. 3 and 5 show the loss-function spectra. Figure 2 shows the optical conductivity spectra of trivalent RB_6 and SmB_6 and Fig. 3 shows the corresponding loss-function spectra. Figure 4 shows the optical conductivity spectra of EuB_6 and YbB_6 together with LaB_6 and Fig. 5 shows the corresponding loss-function spectra. We discuss the origin of the peak structure in the each spectrum in the following section.

III. DISCUSSION

A. Trivalent RB_6 and SmB_6

The profile of the optical conductivity spectra of trivalent RB_6 and SmB_6 shown in Fig. 2 is quite similar

to one another below 21 eV. This means that the structure in these spectra in this energy region is mainly due to the interband transition between the common electronic states to these compounds. LaB_6 has eleven peaks in the energy region below 40 eV; these peak positions are 3.5 eV (*A* peak), 5.3 eV (*B*), 6.8 eV (*C*), 9.0 eV (*D*), 11.0 eV (*E*), 12.5 eV (*F*), 15.0 eV (*G*), 18.0 eV (*H*), 21.0 eV (*I*), 23.5 eV (*J*), and 25.5 eV (*K*). Other materials have the corresponding peaks to LaB_6 in almost the same energy. SmB_6 and GdB_6 have special peaks, labeled *L* at about 14 eV and *M* at about 15 eV, respectively, which overlap with the *F* and *G* peaks.

Let us start to discuss some peak structures which are seen commonly in these materials. According to the results of the energy-band calculation on LaB_6 by Harima *et al.*,[7] the framework of the occupied state is composed of the boron 2*s* and 2*p* bonding states and that of the unoccupied state up to 15 eV from the Fermi level is composed of the rare-earth 5*d* state in addition to the boron 2*s* and 2*p* antibonding states. Beyond 15 eV from the Fermi level, the orthogonalized plane-wave states dominate. The 4*f* state of the rare-earth ion modifies this main structure. In the RB_6, the grade of the modification

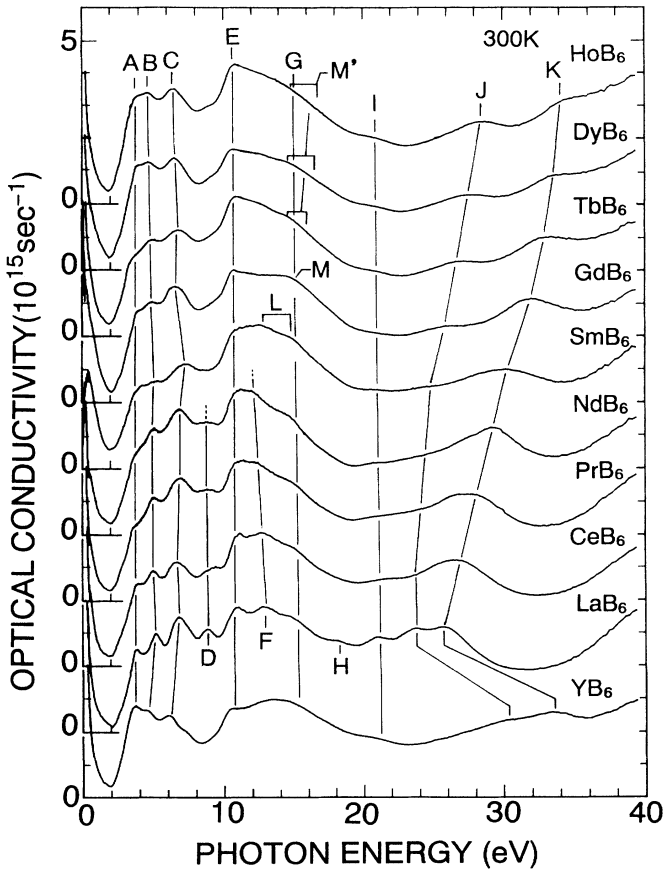

FIG. 2. Optical conductivity [$\sigma(\omega)$] spectra of trivalent rare-earth hexaborides RB_6 (R=Y, La, Ce, Pr, Nd, Gd, Tb, Dy, and Ho) and SmB_6 in the energy region from 1 meV to 40 eV at 300 K. They were obtained from the Kramers-Kronig transformation of the corresponding reflectivity spectra in Fig. 1. See the text for the notation of each peak.

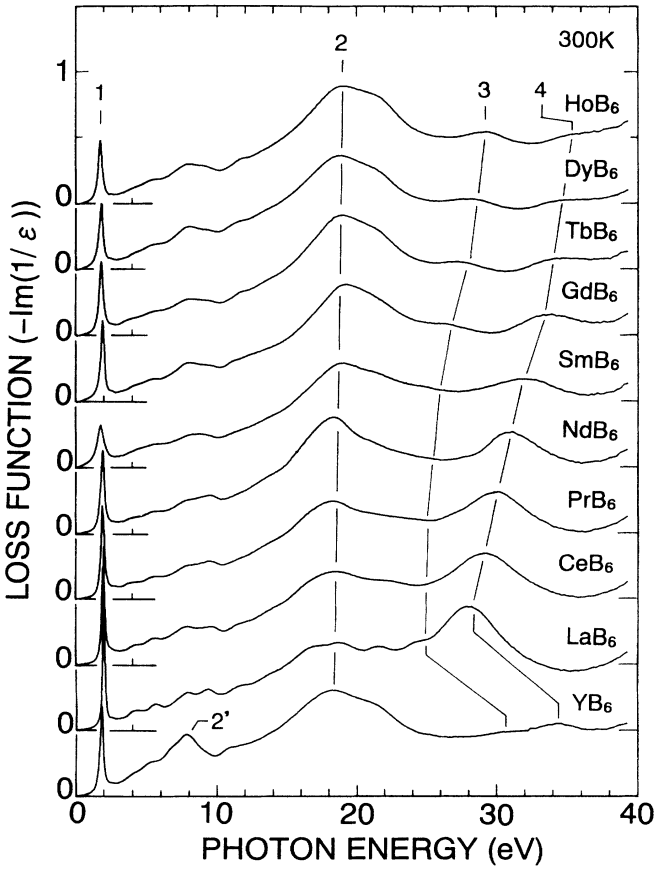

FIG. 3. Loss-function [$-Im(1/\varepsilon)$] spectra of trivalent rare-earth hexaborides RB_6 (R=Y, La, Ce, Pr, Nd, Gd, Tb, Dy, and Ho) and SmB_6 in the energy region between 1 meV and 40 eV at 300 K. See the text for the notation of each peak.

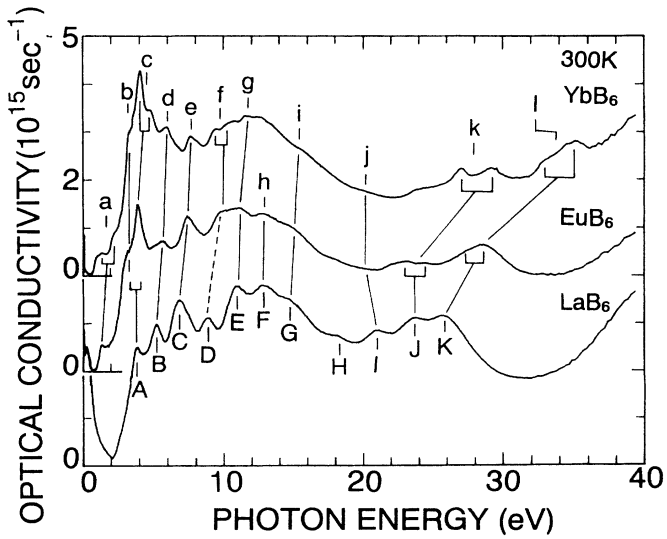

FIG. 4. Optical conductivity [$\sigma(\omega)$] spectra of divalent rare-earth hexaborides RB_6 (R=Eu and Yb) compared with LaB_6 in the energy region from 1 meV to 40 eV at 300 K. See the text for the notation of each peak.

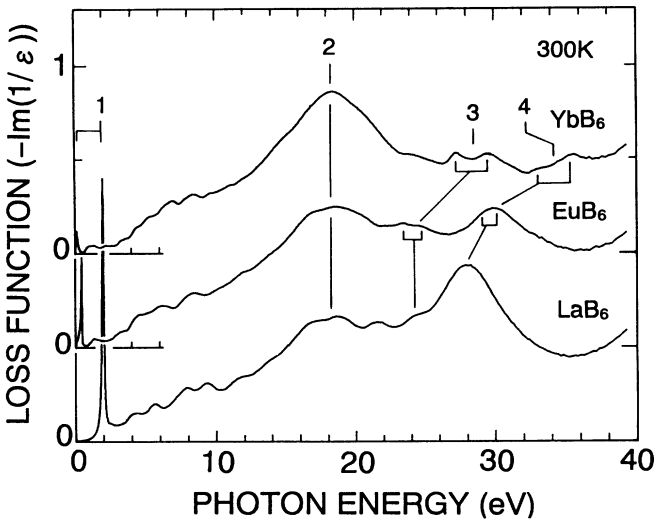

FIG. 5. Loss-function $[-Im(1/\varepsilon)]$ spectra of divalent rare-earth hexaborides RB_6 (R=Eu and Yb) in comparison with LaB_6 in the energy region between 1 meV and 40 eV at 300 K. See the text for the notation of each peak.

of the electronic state by the $4f$ state generates various interesting physical properties. In Fig. 6, we show the density of states (DOS) and the partial DOS of the LaB_6 band calculation shown in a previous publication[8] to make the following discussions clear.

In general, the lattice constant and the band structure of rare-earth compounds are known to change as the $4f$ electron number increases because of the phenomenon known as the lanthanide contraction. However, the change of the lattice constant in RB_6 is small in comparison with other rare-earth compounds such as rare-earth monochalcogenide and rare-earth monopnictide.[15] This is because the crystal structure of RB_6 is constructed by the strong covalent bonding of boron $2s$ and $2p$ states.[3] The main change of the lattice constant is due to the change of the distance between the B_6 and B_6 octahedrons. However, the distance between the boron and boron in the B_6 octahedron changes only a little. Therefore the main band structures of the boron $2s$ and $2p$ bonding and antibonding states within the B_6 octahedron are expected to change very little. However, the bonding and the antibonding bands due to the mixing between the B_6 and B_6 changes systematically with the change of the lattice constant. On the other hand, the magnitude of the screened Coulomb force of the rare-earth atomic core charge acting on a $5d$ state is similar in these materials because the main part of the $5d$ orbital is located outside of the $4f$ orbital. Therefore the similarity of the optical conductivity spectra of trivalent RB_6 and SmB_6 below 21 eV can be understood naturally by the above considerations.

Let us consider the origin of each peak structure in detail. We first discuss the origin of the A peak at about 3.5 eV as shown in Fig. 2. We can see that this peak appears to be in common with all materials. The energy position of this peak corresponds to the energy separation between the top of the occupied state and the bottom of the unoccupied state of the boron $2s$ and $2p$ band in the band calculation.[7] Note, however, that the energy difference in the band calculation is about 1 eV larger than the observed value. The virtual exciton character may be important. In the molecular-orbital picture, the former corresponds to the boron $2s$ and $2p$ bonding states (t_{2g}) and the latter to the bonding orbit between the $5d$ (e_g) state and the boron $2s$ and $2p$ antibonding states (t_{2u}).[3] As shown in the result of the band calculation in Fig. 6, there are no remarkable peak structures on the unoccupied $2s$ and $2p$ antibonding states. Actually, the JDOS calculated between the occupied bonding bands and the unoccupied antibonding bands shows no marked peak.[8] Therefore, hereafter, the other observed peaks are attributed to other characters, the $5d$ bands and the $4f$ bands, which show sharp peaks. It is also important to notice that the boron s character has marked peaks. This is important in the sense that even if its DOS is small compared with the boron p character, it can contribute strongly on the optical absorption because of the boron intra-atomic transition between the $2p$ and the $2s$ states.

It is expected that the B, C, and D peaks are due to the charge-transfer excitation from the boron $2s$ and $2p$ bonding states to the rare-earth $5d$ (t_{2g}) state which is located at about 5 eV above the Fermi level. In our previous papers,[5,8] we could make clear the origin of the C and

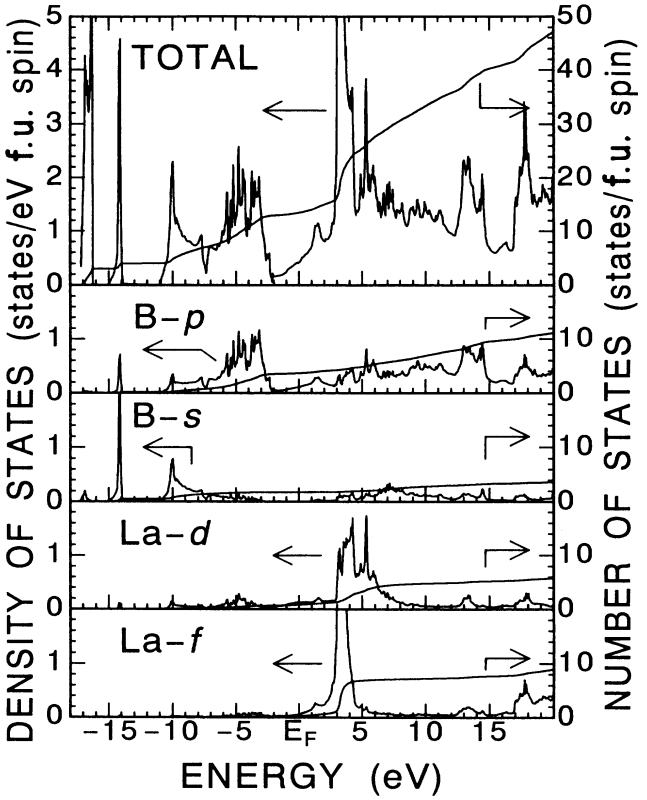

FIG. 6. The total and the partial density of states and these number of states (boron s,p and La d,f) in LaB_6 derived from the model band structure calculation by Harima *et al.* (Ref. 7) in which the unoccupied $4f$ level is shifted upward by 0.10 Ry (1.36 eV) in comparison with the self-consistent augmented plane-wave band structure. For further details of this explanation, see Ref. 8.

D peaks but not the B peak. Now the origin of the B peak can be identified for the first time by our measurement of the reflectivity spectra on YB_6, TbB_6, DyB_6, and HoB_6. At the reference of the band calculation in LaB_6 (Ref. 7) and YB_6,[16] the overlap between the valence band (boron $2s$ and $2p$ bonding states) and the conduction band (rare-earth d state) is larger in YB_6 than in LaB_6. This is due to the fact that in heavy RB_6, including YB_6, the binding energy of the $5d$ electron decreases systematically relative to the boron $2s$ and $2p$ bands. This effect appears in the B, C, and D peaks, i.e., the energy positions of these peaks decrease (the so-called redshift) from LaB_6 to YB_6. YB_6 is a reference material of the heavier RB_6 than GdB_6, because its $4d$ state is similar to the $5d$ state in heavy RB_6 and these lattice constants are also similar to each other. Therefore the same effect is expected to appear in heavier RB_6. This effect is certainly seen in the B, C, and D peaks in heavy RB_6, but only a little. This fact indicates that in RB_6, the energy level of the $5d$ electron changes little relative to the boron $2s$ and $2p$ bands. Note that in the LaB_6 DOS spectrum in Fig. 6, both the bonding $2s$ and $2p$ valence band and the $5d$ band (t_{2g}) split into the doublet structure, which causes three absorption peak structure in agreement with the B-, C-, and D-peak structure. Note also that the D peak in LaB_6 and CeB_6 is sharp and much clearer than that in other RB_6. This suggests that another peak with the above character is overlapping with the D peak. This is considered later. Therefore we can conclude that the origin of all B, C, and D peaks is the charge-transfer excitation from the boron $2s$ and $2p$ bonding states to the rare-earth $5d$ (t_{2g}) state.

It was shown that the mixing of the $4f$ state to the boron $2s$ and $2p$ bonding valence bands is fairly strong which causes the $4f$ (Γ_8) ground state with a large excitation energy for the $4f$ (Γ_7) in CeB_6, but the mixing with the boron $2s$ and $2p$ antibonding state as well as the $5d$ conduction bands is weak.[17] This is consistent with the fact that there is no systematic change for the peak structure in the optical conductivity spectra depending on the energy position of the unoccupied $4f$ state.

It is found that the energy positions of the E, G, and I peaks do not change among all RB_6 but those of the D and F peaks show the redshift and their intensity becomes smaller from LaB_6 to NdB_6 as well as in YB_6. We assign that the transition from the occupied boron $2s$ and $2p$ bonding states to the unoccupied $4f$ state gives these D and F peaks because of the following reasons. It is well known that, as the number of the occupied $4f$ electrons increases, the $4f$ level decreases due to the incomplete Coulomb screening among them. This is the origin of the redshift. In addition, the peak intensity becomes weaker from LaB_6 to NdB_6 as the number of the unoccupied $4f$ state decreases. It is also remarkable that the peak in LaB_6 is particularly sharp. This fact supports the transition to the unoccupied $4f$ state because then we expect a sharp $4f^1$ level in LaB_6 but broadened $4f^n$ peak in other RB_6 and no peak in YB_6. The band calculation shows a substantial mixing of the $4f$ states at the top of the boron $2s$ and $2p$ bonding states, the t_{2g} molecular orbit[7] as was discussed before. Therefore, from the D peak, the unoccupied $4f$ level in LaB_6 is assigned to be about 6 eV above the Fermi level, which is larger than the result of the band calculation.[7] Note that usually the band calculation leaves the unoccupied $4f$ level too low.[18] In LaB_6, the F peak is about 4 eV higher than the D peak. From the band calculation,[7,18] this peak is assigned to be from the bottom of the boron $2s$ and $2p$ bonding states. Note that it is possible to assign these peaks as the intra-atomic d-f transition in which the d characters are mixed into the boron $2s$ and $2p$ bonding state through the d-p mixing effect.

It is remarkable that the intensity of the E and G peaks is strong compared with that of other peaks indicating a strong intra-atomic–allowed transition. In the partial DOS spectrum in Fig. 6, we find a sharp boron s peak at 10 eV below the Fermi level extending to the higher-energy region. Therefore the transition from the boron $2s$ state to the intra-atomic boron $2p$ state in the boron $2s$ and $2p$ unoccupied state of predominantly p character should be the origin of these peaks. The energy position of the E peak corresponds to the energy separation from this boron s peak to the Fermi level and that of the G peak corresponds to the energy separation to the peak of the boron $2s$ and $2p$ antibonding states at about 4 eV above the Fermi level. Then the I peak is naturally identified to the transition to the peak of the boron $2s$ and $2p$ band at 11 eV above the Fermi level. Note that there is another sharp boron $2s$ peak at 14.5 eV below the Fermi level and the same story mentioned above is applicable. Then the energy position of the H peak corresponds to the energy separation from this peak to the boron $2s$ and $2p$ states at about 4 eV above the Fermi level and the origin of the broad peak at about 27 eV common to all RB_6 seems to be due to the transition to the boron $2s$ and $2p$ peaks at 13 ev above the Fermi level in the DOS spectrum.

Next, let us consider the J and K peaks. Their energy positions increase strongly as the number of the occupied $4f$ electrons increases. We can assign that the J and K peaks are due to the transition from the spin-orbit doublet of the rare-earth $5p$ core state to the $5d$ (t_{2g}) state. For example, the spin-orbit doublet of the $5p$ state of LaB_6 is known to be located at 18 eV ($5p_{3/2}$) and 20 eV ($5p_{1/2}$) below the Fermi level by the resonant ultraviolet photoemission spectroscopy (UPS) data by Aono *et al.*[19] In the DOS spectrum it appears at 16.5 eV below the Fermi level as shown in Fig. 6. The peak of the $5d$ (t_{2g}) state is located at about 5 eV above the Fermi level as we have described before in relation to the assignment of peaks B, C, and D. Therefore the interband transitions from the $5p_{3/2}$ and $5p_{1/2}$ to the $5d$ (t_{2g}) states give two peaks at 23 and 25 eV. These transition energy positions are very close to those of the J and K peaks. In addition, the energy separation between this spin-orbit doublet is in good agreement with the energy difference of the J and K peaks. This result holds also for CeB_6 and PrB_6. From the resonant UPS data on CeB_6 and PrB_6 by Sugawara *et al.*,[20] the spin-orbit doublet structure of the $5p$ state is located at 18.5 eV ($5p_{3/2}$) and 22 eV ($5p_{1/2}$) in CeB_6 and 19 eV ($5p_{3/2}$) and 23 eV ($5p_{1/2}$) in PrB_6, respectively,

below the Fermi level. The observed energy difference between the J and K peaks is also consistent with the UPS data of CeB_6 and PrB_6. In other materials, the J and K peaks shift to the higher-energy side (the so-called blueshift) and the spin-orbit splitting energy increases as the atomic number of rare-earth ion increases. This means that the energy position of the $5p$ core state becomes deeper and the spin-orbit splitting energy between the $5p_{1/2}$ and $5p_{3/2}$ levels becomes larger as the atomic number of the rare-earth ion increases. The splitting energy of the $5p$ core level is decided as 3.5 eV in YB_6, 2.0 eV in LaB_6, 3.5 eV in CeB_6, 4.0 eV in PrB_6, 4.5 eV in NdB_6, 5.6 eV in SmB_6, 6.0 eV in GdB_6, 6.0 eV in TbB_6, 6.0 eV in DyB_6, and 6.0 eV in HoB_6. These values will be observed by the photoelectron spectroscopy.

In our previous paper,[5] we have already assigned the L and M peaks in SmB_6 and GdB_6 to the transitions from the occupied $4f$ to the $5d$ (t_{2g}) states. The $4f$-$5d$ transition should also exist in other RB_6. Actually, in comparison with the spectrum of LaB_6, there is an extra broad and unclear structure with the center at about 8 eV, 10 eV in PrB_6 and NdB_6, respectively, overlapping with the C, D, and E peaks. The peak positions are consistent with the energy separation between the unoccupied $5d$ (t_{2g}) level as mentioned above and the occupied $4f$ level of the x-ray photoemission spectroscopy (XPS) data by Champagna *et al.*[21] The broadening of this structure in the optical conductivity spectra is also consistent with the data of the occupied $4f$ state of the XPS. This means that the reason for the broadening of the $4f$-$5d$ transition structure is due to the broadening of the occupied $4f$ state. This reason for this is thought to be that the final $4f^{n-1}$ state has a multiplet structure and furthermore has lifetime broadening with the occupied boron $2s$ and $2p$ states, i.e., the mixing effect between the boron $2s$ and $2p$ bonding states and the occupied rare-earth $4f$ state. The situation is more complicated in heavy RB_6 because there are two kinds of occupied $4f$ states, the majority up-spin state with deeper binding energy and the minority down-spin $4f$ state with shallower energy. In TbB_6, DyB_6, and HoB_6, the former corresponds to the L and M peaks and shows blueshift. The latter corresponds to the broad structure due to the transition from the $4f$ state in PrB_6 and NdB_6 and also shows blueshift. Naturally they should show broad structures. Actually we can identify these peaks by subtracting the result for LaB_6. The former structure can be seen more clearly as shown by M' in Fig. 2. Note that the peak for GdB_6 is sharpest because of the lower energy splitting in the final $4f^{n-1}$ state.[21] It is possible to estimate the $4f$-$5d$ oscillator strength in GdB_6 to be about 0.5 as mentioned in our previous paper.[5] Note that is it expected that the unoccupied $4f$ states in CeB_6, PrB_6, and NdB_6 are spin-orbit split into the up-spin state and the down-spin state where the latter have more states and the splitting energy becomes larger as the number of occupied $4f$ states increases. However it is difficult to estimate the amount of splitting because of its relatively weak intensity of the absorption structure to these states.

Loss-function spectra shown in Fig. 3 confirm the above assignment. Four large peak structures labeled 1, 2, 3, and 4 appear in the spectra. It is obvious that peak 1 shows the excitation of the plasmon of the conduction electron. Peak 2 can be assigned to the excitation of the plasmon of the valance band which consists of the boron $2s$ and $2p$ bonding state including the occupied $4f$ state. Peaks 3 and 4 are due to the $5p_{3/2}$ and the $5p_{1/2}$ absorption, respectively. In YB_6, the peak at 8 eV labeled 2′ exists. This is thought to be the plasmon of the boron $2s$ and $2p$ bonding states up to the gap at 7.5 eV below the Fermi level in Fig. 6. In other RB_6's, too, we can see this peak even though it is not so clear.

B. Divalent RB_6

Figure 4 shows the optical conductivity spectra of EuB_6 and YbB_6 in comparison with LaB_6. EuB_6 are YbB_6 are known as divalent RB_6's. In EuB_6, 12 peaks appeared at the energy position of 1.0 eV (a peak), 3.0 eV (b), 4.0 eV (c), 5.2 eV (d), 7.5 eV (e), 10.0 eV (f), 11.5 eV (g), 13.0 eV (h), 15.0 eV (i), 20.0 eV (j), 22.5 eV (k), and 28.0 eV (l). In YbB_6, we can see several peaks that correspond to those of EuB_6. Both EuB_6 and YbB_6 have a characteristic structure below 4 eV that is different from LaB_6, but the other structure is almost the same as that of LaB_6. This fact confirms that the main profile of the spectrum of the divalent RB_6 compound is determined by the similar interband transition from the boron $2s$ and $2p$ bonding states to the boron $2s$ and $2p$ antibonding states and to the rare-earth $5d$ state with trivalent RB_6. It is clear that the boron $2s$ and $2p$ bonding and antibonding band structure does not depend on the valence of rare-earth ion nor the energy position of the Fermi level. Therefore we expect the same absorption structure in all RB_6's. On the other hand, the $5d$ level is pushed up by about 1–2 eV relative to the boron $2s$ and $2p$ bands. This causes the overlapping of the boron $2s$ and $2p$ bonding bands and the conduction band is nearly zero and thus puts the Fermi level at the top of the valence band. Because of the insulator character, some exciton peaks are expected. Based on the above picture we analyze the data for EuB_6 and YbB_6 in detail compared with LaB_6. At first, we discuss the common structures seen in LaB_6, EuB_6, and YbB_6.

In LaB_6, the origins of the B, C, and D peaks were attributed to the transition from the boron $2s$ and $2p$ bonding states to the La $5d$ (t_{2g}) state. The corresponding peaks (labeled d, e, and f) show the blueshift, respectively, by 0.3 eV in EuB_6 and 0.7 eV in YbB_6, as we expected. It is also clear that another type of peak is overlapping at the f- peak.

It seems that main part of the f peak is due to the transition from the occupied $4f$ to the $5d$ (t_{2g}) states in Eu^{2+} and Yb^{2+} for the following reason. The unoccupied $5d$ (t_{2g}) state of LaB_6 is located at about 5 eV above the Fermi level. The Fermi level of EuB_6 and YbB_6 is located at the lower energy position by 1–2 eV than that of LaB_6 relative to the boron $2s$ and $2p$ bands. The occupied $4f$ level of both materials stays about 1–2 eV below the Fermi level according to the photoelectron data by Taka-

kuwa *et al.* for EuB_6 (Ref. 22) and Iga *et al.* for YbB_6.[23] Considering the blueshift of about 1 eV in the $5d$ level from LaB_6 to these divalent RB_6's, the energy separation between the occupied $4f$ and the unoccupied $5d$ (t_{2g}) states is expected to be about 9 eV in both materials. This energy separation is consistent with the observed energy position of the f peak. Furthermore, the strong absorption intensity is consistent with the large oscillator strength of the intra-atomic $4f$-$5d$ transition as estimated before.[5] The f peak in YbB_6 has a doublet structure. This is also consistent with the $4f$ spin-orbit doublet in YbB_6 of about 1 eV observed by UPS.[23]

Both EuB_6 and YbB_6 possess characteristic structures below 4 eV which do not exist in trivalent RB_6. The detailed experimental[24] and theoretical[25] studies on europium chalcogenide compounds EuX (X=O, S, Se, and Te) give useful information for EuB_6. First, we refer to EuX.

The Eu chalcogenides form NaCl-type crystal structures and Eu is divalent. Therefore the p band of the chalcogen ion is occupied perfectly and the $5d$ band of the Eu ion is unoccupied. The energy gap between the valence (chalcogen p state) and the conduction (Eu $5d$ state) bands is about 2–5 eV. The occupied $4f$ level with up-spin exists in the main gap. Therefore the lowest absorption band is due to the intra-atomic transition from the $4f$ to the $5d$ states in the Eu ion. In the metallic states in which some $5d$ bands are occupied, the created $4f$ hole is screened by other $5d$ band electrons and thus the excited $5d$ electron is not trapped to the $4f$ hole but makes a $5d$ band. Therefore in metals such as trivalent RB_6, we observe the $4f$-$5d$ transition. In the insulator such as EuX, the $4f$ hole is not completely screened and thus the excited $5d$ electron is trapped to the $4f$ hole. This is the magnetic exciton state studied in detail in EuX.[24,25] When the $5d$ electron is completely trapped at the same ion as the $4f$ hole, all of the $4f$-$5d$ transition becomes an exciton. Because the excited $5d$ electron is, however, usually extended to the neighbor sites, the $4f$-$5d$ transition splits into the exciton peak and the transition to the $5d$ band in which the ratio of the exciton transition is proportional to the ratio of the excited $5d$ electron sitting at the $4f$ hole site, which is about a half in EuX.

The same situation is expected in EuB_6 and YbB_6. However, the situation is more complicated because the $4f$ hole level overlaps with the top of the borons $2s$ and $2p$ bonding states and the $5d$ levels overlap with the lower part of the boron $2s$ and $2p$ antibonding bands. This means that the $4f$-$5d$ exciton and the boron $2s$ and $2p$ bonding-antibonding excitons as well as the $2s$ and $2p$ bonding-state–$5d$ exciton coexist and interact with each other forming more complicated exciton structures. Actually, this strong and complicated exciton structure is observed both in EuB_6 and YbB_6 as the a, b, and c peaks, and is much stronger than the A peak in LaB_6. It should be noted that, compared with EuB_6, the a and c peaks in YbB_6 have doublet structures with similar splitting as the $4f$ spin-orbit splitting mentioned before. This fact seems to suggest that the a peak is predominantly a $4f$-$5d$ (e_g)-type symmetry exciton of the fairly extending $5d$ (e_g) state and the c peak is the $4f$-$5d$ (t_{2g}) state of the localized character of the $5d$ (t_{2g}) state.

The E, F, and G peaks in LaB_6 also appear in EuB_6 and YbB_6 in the nearly same energy region, although the E peak overlaps with the peak structure due to the $4f$-$5d$ transition as mentioned before and is thus not clear.

It is obvious that the k and l peaks are due to the transition from the $5p_{3/2}$ and $5p_{1/2}$, states, respectively, to the $5d$ (t_{2g}) state which corresponds to the J and K peaks in LaB_6. The spin-orbit splitting energy between the $5p_{1/2}$ and $5p_{3/2}$ states is about 4.5 eV in EuB_6 and 6.0 eV in YbB_6. In these spectra, it is seen that both the k and l peaks have the doublet structure with an energy difference of 1.5 eV in EuB_6 and 2.0 eV in YbB_6. This splitting structure seems to be caused by the two-peak structure of the $5d$ (t_{2g}) band as mentioned before. Due to the nonmetallic character of EuB_6 and YbB_6, the intra-atomic exciton character of the $5p$-$5d$ transition is much clearer in the present materials causing a sharper structure.

Loss-function spectra in Fig. 5 confirm the assignment as mentioned above. It is obvious that peak 1 corresponds to the plasmon of conduction electron. The energy positions of peak 1 of EuB_6 and YbB_6 are reduced strongly from that of LaB_6 because the number of conduction electrons in EuB_6 and YbB_6 is much smaller than that in LaB_6. Peak 2 shows the plasmon of the valence band including the occupied $4f$ band and peaks 3 and 4 show the transition or exciton from the $5p_{3/2}$ and $5p_{1/2}$ states, respectively.

IV. CONCLUSIONS

Reflectivity spectra of all rare-earth hexaborides RB_6 (R=La, Ce, Pr, Nd, Sm, Eu, Gd, Tb, Dy, Ho, Yb, and Y), in which interesting valence fluctuating materials, CeB_6 and SmB_6, are involved, were measured in the energy region from 1 meV to 40 eV. The electronic state of RB_6 was investigated by the analysis of the optical conductivity and the loss-function spectra which were obtained from the Kramers-Kronig transformation of the reflectivity spectrum. The following results were obtained. (1) For the trivalent RB_6 including SmB_6, LaB_6 and YB_6 were chosen as the reference materials for the light and heavy RB_6 without occupied $4f$ electrons, respectively. From different spectra we can obtain the $4f$ contribution. (2) Except for the $4f$ contribution, the observed spectra could be explained very well by the LaB_6 band calculation, in which the partial DOS for the boron s and p and the rare-earth d and f are shown separately. (3) It was shown that the boron $2s$ and $2p$ bonding and antibonding bands seem not to change in all the RB_6's even though the lattice distance changes. The calculated JDOS between the boron $2s$ and $2p$ bonding and antibonding bands has no remarkable peaks. This seems to be consistent with the experimental results. The main peaks are identified as the sharp peaks in the boron $2s$ and the rare-earth $5d$ and $4f$ characters. (4) The spectra of SmB_6 is essentially equal to other trivalent RB_6's except for a small blueshift of the $5d$ bands. The spectra of CeB_6 is essentially equal to other trivalent RB_6's. (5) It

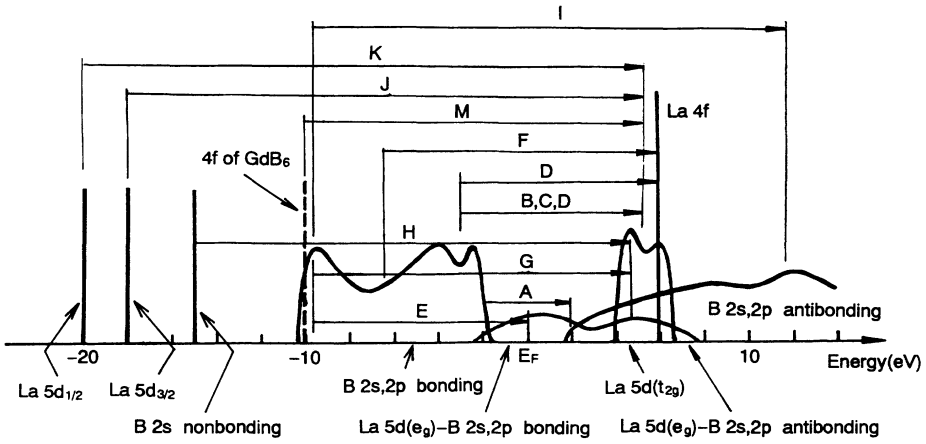

FIG. 7. The schematic figure of the electronic structure and optical transitions of LaB_6 and $4f$ state of GdB_6 estimated by the optical conductivity spectra in Figs. 2 and 4. The indexes $A-M$ mean the optical transitions of the origin of the peaks $A-M$ in Fig. 2.

was possible to identify the occupied $4f$ levels due to the strong intra-atomic $4f$-$5d$ transition. They show a smooth systematic change as expected, consistent with the photoelectron results. On the other hand, the unoccupied $4f$ level position was not so clearly observed due to the weak intensity of the transition to this state. (6) In the divalent semiconducting materials EuB_6 and YbB_6, strong complex exciton peaks were found at the absorption edge below 4 eV. These origins are thought to be the mixture of the $4f$-$5d$ exciton and the excitons from the boron $2s$ and $2p$ bonding state to the $2s$ and $2p$ antibonding and the $5d$ states. The blueshifts of the $5d$ bands from LaB_6 to EuB_6 and YbB_6 are also observed. In these divalent RB_6's the occupied $4f$ levels were found at about 1 eV below the Fermi level to the consistent with other experiments. (7) In all RB_6's the transition from the $5p$ to the $5d$ (t_{2g}) states was observed and the structure due to the spin-orbit splitting between the $5p_{3/2}$ and the $5p_{1/2}$ states was clearly revolved in the spectrum.

From these conclusions, a schematic figure of the electronic structure and optical transitions of LaB_6 which were estimated by the optical conductivity spectra was shown in Fig. 7.

ACKNOWLEDGMENTS

The authors would like to thank Professor T. Ishii and the staff of SOR-RING of the Institute for Solid State Physics, the University of Tokyo. They especially thank Dr. M. Fujisawa for his advice on the measurements at the beam line BL-1 of the SOR-RING. One of the authors (S. Kimura) gratefully acknowledges useful discussions with Professor M. Ikezawa of Tohoku University and Dr. H. Harima of the University of Osaka Prefecture, and also thanks The Kasuya Research Foundation for financial support. This research was supported in part by a Grant-in-Aid for Scientific Research by the Ministry of Education, Science and Culture of Japan.

[1]e.g., T. Kasuya, M. Kasaya, K. Takegahara, T. Fujita, T. Goto, A. Tamaki, M. Takigawa, and H. Yasuoka, J. Magn. Magn. Mater. **31-34**, 447 (1983).

[2]e.g., T. Komatsubara, N. Sato, S. Kunii, I. Oguro, Y. Furukawa, Y. Onuki, and T. Kasuya, J. Magn. Magn. Mater. **31-34**, 368 (1983).

[3]H. C. Longuet-Higgins and M. de V. Roberts, Proc. R. Soc. London **224**, 336 (1954).

[4]G. Travaglini and P. Wachter, Phys. Rev. B **29**, 893 (1984).

[5]S. Kimura, T. Nanba, S. Kunii, and T. Kasuya, J. Phys. Soc. Jpn. **59**, 3388 (1990).

[6]S. Kimura, T. Nanba, S. Kunii, T. Suzuki, and T. Kasuya, Solid State Commun. **75**, 717 (1990).

[7]H. Harima, O. Sakai, T. Kasuya, and A. Yanase, Solid State Commun. **66**, 603 (1988).

[8]S. Kimura, H. Harima, T. Nanba, S. Kunii, and T. Kasuya, J. Phys. Soc. Jpn. **60**, 745 (1991).

[9]T. Nanba, H. Ohta, R. Tanaka, M. Motokawa, S. Kimura, S. Kunii, and T. Kasuya, Physica B (to be published).

[10]S. Kimura, T. Nanba, S. Kunii, and T. Kasuya (unpublished).

[11]T. Tanaka, E. Bannai, S. Kawai, and T. Yamane, J. Cryst. Growth **30**, 193 (1975).

[12]T. Nanba, Y. Urashima, M. Ikezawa, M. Watanabe, E. Nakamura, K. Fukui, and H. Inokuchi, Int. J. Infrared Millimeter Waves **7**, 1769 (1986); T. Nanba, Rev. Sci. Instrum. **60**, 1680 (1989).

[13]F. Wooten, *Optical Properties of Solids* (Academic, New York, 1972).

[14]M. Cardona and D. L. Greenaway, Phys. Rev. **133**, A1685 (1964); M. Cardona, *ibid.* **140**, A651 (1965).

[15]See, e.g., S. Kimura, Doctor thesis (in Japanese), Tohoku University, 1990.

[16]Y. Aoki, Doctor thesis (in Japanese), Tohoku University, 1982.

[17]M. Ikeda, Y. Aoki, and T. Kasuya, J. Magn. Magn. Mater. **52**, 264 (1985).

[18]A. Hasegawa and A. Yanase, J. Phys. F **7**, 1245 (1977).

[19]M. Aono, T.-C. Chiang, J. A. Knapp, T. Tanaka, and D. E.

Eastman, Phys. Rev. B **21**, 2661 (1980).

[20]H. Sugawara, A. Kakizaki, I. Nagakura, T. Ishii, T. Komatsubara, and T. Kasuya, J. Phys. Soc. Jpn. **51**, 915 (1982).

[21]M. Champagna, G. K. Wertheim, and Y. Bear, in *Photoemission in Solids II*, edited by L. Ley and M. Cardona (Springer-Verlag, Berlin, 1979), p. 217; J.-N. Chazalviel, M. Champagna, G. K. Wertheim, P. H. Schmidt, and Y. Yafet, Phys. Rev. Lett. **37**, 919 (1976).

[22]Y. Takakuwa, S. Suzuki, and T. Sagawa, Jpn. J. Appl. Phys. Suppl. **17-2**, 284 (1978).

[23]F. Iga, Y. Takukuwa, T. Takahashi, M. Kasaya, T. Kasuya, and T. Sagawa, Solid State Commun. **50**, 903 (1984).

[24]T. Mitani, M, Ishibashi, and T. Koda, J. Phys. Soc. Jpn. **38**, 731 (1975); T. Mitani and T. Koda, Phys. Rev. B **12**, 2311 (1975).

[25]O. Sakai, A. Yanase, and T. Kasuya, J. Phys. Soc. Jpn. **42**, 596 (1977).